

Evidence for a Novel K^+ Channel Modulated by α_{1A} -Adrenoceptors in Cardiac Myocytes

Stéphanie C. M. Choisy, Jules C. Hancox, Lesley A. Arberry, A. Martyn Reynolds,¹ Michael J. Shattock, and Andrew F. James

Department of Physiology and Cardiovascular Research Laboratories, School of Medical Sciences, University of Bristol, Bristol, United Kingdom (S.C.M.C., J.C.H., L.A.A., A.F.J.); Department of Renal Medicine, King's College School of Medicine & Dentistry, London, United Kingdom (A.M.R.); and Cardiac Physiology, Centre for Cardiovascular Biology & Medicine, St Thomas' Hospital, London, United Kingdom (M.J.S.)

Received March 25, 2004; accepted June 22, 2004

ABSTRACT

Accumulating evidence suggests that steady-state K^+ currents modulate excitability and action potential duration, particularly in cardiac cell types with relatively abbreviated action potential plateau phases. Despite representing potential drug targets, at present these currents and their modulation are comparatively poorly characterized. Therefore, we investigated the effects of phenylephrine [PE; an α_1 -adrenoceptor (α_1 -AR) agonist] on a sustained outward K^+ current in rat ventricular myocytes. Under K^+ current-selective conditions at 35°C and whole-cell patch clamp, membrane depolarization elicited transient (I_t) and steady-state (I_{ss}) outward current components. PE (10 μ M) significantly decreased I_{ss} amplitude, without significant effect on I_t . Preferential modulation of I_{ss} by PE was confirmed by intracellular application of the voltage-gated K^+ channel blocker tetraethylammonium, which largely inhibited I_t without affecting the PE-sensitive current ($I_{ss,PE}$). $I_{ss,PE}$ had the proper-

ties of an outwardly rectifying steady-state K^+ -selective conductance. Acidification of the external solution or externally applied $BaCl_2$ or quinidine strongly inhibited $I_{ss,PE}$. However, $I_{ss,PE}$ was not abolished by anandamide, ruthenium red, or zinc, inhibitors of TASK acid-sensitive background K^+ channels. Furthermore, the PE-sensitive current was partially inhibited by external administration of high concentrations of tetraethylammonium and 4-aminopyridine, which are voltage-gated K^+ channel-blockers. Power spectrum analysis of $I_{ss,PE}$ yielded a large unitary conductance of 78 pS. $I_{ss,PE}$ resulted from PE activation of the α_{1A} -AR subtype, involved a pertussis toxin-insensitive G-protein, and was independent of cytosolic Ca^{2+} . These results collectively demonstrate that α_{1A} -AR activation results in the inhibition of an outwardly rectifying steady-state K^+ current with properties distinct from previously characterized cardiac K^+ channels.

The exceptional diversity of K^+ channels has particular significance in the heart, where different currents contribute to distinct phases of the cardiac action potential (Snyders, 1999). Steady-state, or plateau, currents show very rapid activation and relatively slow or no inactivation and thereby contribute outward current through out phases 1 and 2, and

for the early part of phase 3 of the action potential. They are therefore thought to be of particular importance in cardiac cell types with relatively abbreviated plateau phases (Nattel et al., 1999; Snyders, 1999). However, compared with the transient outward (I_{to1}) and delayed rectifier (I_K) K^+ currents, little is known about the steady-state currents and their modulation (Nattel et al., 1999; Snyders, 1999).

The steady-state currents represent a diverse family that includes the so-called ultra-rapid delayed rectifiers (I_{Kur}) of mouse ventricular myocytes and human and canine atrial myocytes (Nattel et al., 1999). Although I_{Kur} are themselves molecularly diverse, in that they are composed of $Kv1.2$,

This work was supported by the British Heart Foundation (PG/98091 and PG/03/073) and the Wellcome Trust.

¹ Current address: Cairn Research Ltd, Graveney Road, Faversham, Kent, ME13 8UP, U.K.

Article, publication date, and citation information can be found at <http://molpharm.aspetjournals.org>.
doi:10.1124/mol.104.000760.

ABBREVIATIONS: 4-AP, 4-aminopyridine; TEA, tetraethylammonium; Slick, sequence like an intermediate conductance K^+ channel; TASK, two-pore domain acid-sensitive K^+ channel; TREK, two-pore domain-related K^+ channel; α_1 -AR, α_1 -adrenoceptor; PE, phenylephrine; MAFP, methylarachidonyl fluorophosphonate; PKC, protein kinase C; U73122, 1-[6-((17 β -3-methoxyestra-1,3,5(10)-trien-17-yl)amino)hexyl]-1H-pyrrole-2,5-dione; U73343, 1-[6-((17 β -3-methoxyestra-1,3,5(10)-trien-17-yl)amino)hexyl]-1H-2,5-pyrroledione; AACOCF₃, arachidonyl tri-fluoromethylketone; A61603, N-(5-[4,5-dihydro-1H-imidazole-2-yl]-2-hydroxy-5,6,7,8-tetrahydronaphthalen-1-yl) methane sulphonamide hydrobromide; WB4101, 2-(2',6'-dimethoxyphenoxyethyl)-aminomethyl-1,4-benzodioxan; CEC, chloroethylclonidine; BAPTA, 1,2-bis(2-aminophenoxy)ethane-*N,N,N',N'*-tetraacetic acid; GDP β S, guanosine 5'-[β -thio]diphosphate; CP, conditioning potential; PTX, pertussis toxin; PLC, phospholipase C; PLA, phospholipase A; PKC, protein kinase C; PI 3-kinase, phosphatidylinositol 3-kinase.

Kv1.5, Kv2.1, or Kv3.1 voltage-gated K^+ channel α -subunits, they are distinguished from other steady-state currents by their sensitivity to the K^+ channel blocker, 4-aminopyridine (4-AP; IC_{50} 5–50 μ M) (Nattel et al., 1999). Other, less well characterized, steady-state currents include I_{Kp} of guinea pig ventricular myocytes and I_{ss} of rat atrial and ventricular myocytes (Apkon and Nerbonne, 1991; Backx and Marban, 1993; van Wagoner et al., 1996; Himmel et al., 1999). Rat I_{ss} is at least an order of magnitude less sensitive to 4-AP than is I_{Kur} (Apkon and Nerbonne, 1991; Himmel et al., 1999). Rat I_{ss} is also only partially inhibited by external application of tetraethylammonium (TEA), another voltage-gated K^+ channel blocker (Himmel et al., 1999; Snyders, 1999).

Slick (Sequence Like an Intermediate Conductance K^+ channel, or slo 2.1) is a rapidly activating, large-conductance, voltage-gated K^+ channel that has recently been shown to be selectively expressed in the brain and the heart (Bhattacharjee et al., 2003). So far, no endogenous currents for Slick have been identified. However, in principle, because it produces relatively sustained outward currents that are partially sensitive to external TEA, Slick could contribute to cardiac steady-state K^+ currents (Bhattacharjee et al., 2003). Likewise, the recently identified two-pore domain K^+ channels (K_{2P}) channels that form almost instantaneous, noninactivating background outward currents could also contribute to cardiac steady-state currents (Lesage and Lazdunski, 2000). mRNA and protein for TASK-1, an acid-sensitive K_{2P} channel thought to play a role in the modulation of membrane excitability by G-protein-coupled receptor stimulation in neuronal cells (Millar et al., 2000; Talley et al., 2000) have been isolated from the heart (Duprat et al., 1997; Leonoudakis et al., 1998; Kim et al., 1999; Barbuti et al., 2002; Jones et al., 2002). Therefore, it has been suggested that TASK-1 channels contribute to the modulation of cardiac excitability and refractoriness (Duprat et al., 1997; Leonoudakis et al., 1998; Kim et al., 1999; Barbuti et al., 2002; Jones et al., 2002). Furthermore, TREK-1, an outwardly rectifying mechanosensitive K_{2P} channel activated by membrane stretch or polyunsaturated fatty acids, is thought to underlie a G-protein-coupled receptor-modulated arachidonic acid-sensitive current, I_{KAA} , in rat cardiac myocytes (Patel et al., 1998; Aimond et al., 2000; Terrenoire et al., 2001).

Many cardiac K^+ currents, including the inward rectifier (I_{K1}), transient outward current (I_{to1}), and ultrarapidly activating outward rectifier (I_{Kur}) currents are modulated by α_1 -adrenoceptor (α_1 -AR) stimulation (Fedida et al., 1993a; Nattel et al., 1999). In addition, there is evidence that the α_1 -AR agonist phenylephrine (PE), inhibits a relatively sustained outward current in rat cardiac myocytes (Ravens et al., 1989; Ertl et al., 1991; van Wagoner et al., 1996). Although the properties of this current are unclear, it has previously been suggested to represent a subtype of the voltage-gated K^+ current, I_{Kur} (van Wagoner et al., 1996; Nattel et al., 1999). Three subtypes of α_1 -AR, α_{1A} , α_{1B} , and α_{1D} , are expressed in the rat ventricle (Homma et al., 2000), and different receptor subtypes coupling with separate signaling pathways have been shown to modulate distinct canine ventricular K^+ currents (Wang et al., 2001). The objectives of this study, therefore, were 1) to examine the properties of PE-sensitive K^+ currents of rat ventricular myocytes, with particular emphasis on steady-state current and 2) to estab-

lish the receptor signaling pathways mediating the predominant effects of α_1 -AR stimulation.

Materials and Methods

Drugs and Reagents. Anandamide, chelerythrine, genistein, bisindolylmaleimide I (GF109203X), methylarachidonyl fluorophosphate (MAFP), neomycin sulfate, pertussis toxin, PKC ϵ inhibitor peptide, staurosporine, U73122, U73343, and wortmannin were purchased from Calbiochem (Nottingham, UK), arachidonyl tri-fluoromethylketone (AACOCF₃) and the G_q -protein antagonist peptide GP2A were from Biomol (Exeter, UK), and A61603 and WB4101 were from Tocris (Bristol, UK). All other reagents were purchased from Sigma (Poole, UK).

A61603, atenolol, carbachol, chloroethylclonidine (CEC), isoprenaline, neomycin sulfate, pertussis toxin, PE, and WB4101 were dissolved at 1000 times final concentration in de-ionized water (dH₂O) immediately before use. In this study, 10 μ M PE was used as a maximally effective concentration of the α_1 -AR agonist (Fedida et al., 1993a). The PKC ϵ inhibitor and the GP2A G_q -protein antagonist peptides were dissolved in dH₂O and stored at -20°C until use. Nifedipine and prazosin were stored at 4°C as stock solutions of at least 1000 times the final concentration in ethanol. To avoid oxidation during storage, AACOCF₃, anandamide, MAFP, U73122, and U73343 were aliquoted to the appropriate amounts for experimental use by solution in chloroform under a nitrogen atmosphere, and all chloroform evaporated before storage at -20°C . Before addition to experimental solutions, these reagents were dissolved in ethanol or dimethyl sulfoxide to at least 1000 times the final concentration. External experimental solutions containing 4-AP, TEA, and quinidine were made up at the final concentration immediately before use. The 50 mM TEA solution was made by equimolar replacement of NaCl with TEA. All other reagents were dissolved in dimethyl sulfoxide to at least 1000 times the final concentration, aliquoted, and stored at -20°C until use.

Myocyte Isolation. Male Wistar rats (200–250g) were killed humanely according to UK government legislation. The heart was excised rapidly and mounted on a Langendorff apparatus and retrogradely perfused via the aorta with a series of solutions, at 37°C , based on an isolation solution comprising 130 mM NaCl, 5.4 mM KCl, 1.4 mM MgCl₂, 0.4 mM NaH₂PO₄, 4.2 mM HEPES, 10 mM D-glucose, 20 mM taurine, and 10 mM creatine, pH 7.3. Hearts were initially perfused for 2 to 4 min with a solution containing 750 μ M CaCl₂. The heart was then perfused for 4 min with a Ca^{2+} -free isolation solution containing 100 μ M EGTA; this was followed by perfusion with isolation solution containing 1 mg/ml Worthington type 2 collagenase (Lorne Laboratories, Reading, UK), 0.1 mg/ml protease (type XIV; Sigma), and 0.1% dialyzed bovine serum albumin (Sigma A-6003). After 8 min, the heart was removed from the apparatus, and the left ventricular free wall was finely chopped and gently agitated in fresh enzyme-containing solution at 37°C . The tissue was agitated for 4-min periods, after which the tissue was filtered through nylon gauze to separate dissociated cells from the remaining undigested tissue. The undigested tissue was then further treated with fresh enzyme solution. Dissociated cells were sedimented by centrifugation and re-suspended in Ca^{2+} -free isolation solution. The cells were then resedimented and resuspended three times; at each resuspension, the Ca^{2+} was incremented to a final concentration of 750 μ M. Cells were stored in this Ca^{2+} -containing isolation solution at room temperature and used within 9 h of isolation.

Whole-Cell Recording. Cells were superfused with an external solution comprising 134 mM NaCl, 4 mM KCl, 1.2 mM MgCl₂, 1 mM CaCl₂, 10 mM HEPES, and 11 mM D-glucose, pH 7.35 at 35°C . Nifedipine (3 μ M) and atenolol (1 μ M) were added to block L-type Ca^{2+} currents and β -adrenoceptors, respectively. K^+ -free external solution was produced by equimolar replacement of KCl with CsCl. Pipettes were pulled from borosilicate glass capillaries (Corning

8250; A-M Systems, Sequim, WA) to tip resistances of 1.5 to 3.0 MΩ. Perforated patch recordings were made using a pipette solution comprising 125 mM HCH₃O₃S, 125 mM KOH, 10 mM KCl, 5 mM NaCl, 5 mM MgCl₂, and 10 mM HEPES, pH 7.2 (KOH) to which 225 μg/ml amphotericin B was added according to a recipe kindly provided by Dr. Andy Trafford (Manchester, UK). Conventional whole-cell recordings were made using a pipette solution containing 130 mM HCH₃O₃S, 130 mM KOH, 10 mM KCl, 10 mM EGTA, 2 mM MgCl₂, 1 mM CaCl₂, 10 mM HEPES, 4 mM MgATP, and 0.2 mM Na₂GTP, pH 7.2 (KOH). The free Ca²⁺ concentration of this solution was calculated to be ~25 nM using WCaBuf software kindly provided by Dr. Guy Droogmans (Leuven, Belgium). For the majority of experiments, a low concentration of Na⁺ was used to minimize the contribution of Na⁺-dependent electrogenic transporters (i.e., Na⁺/K⁺ ATPase and Na⁺/Ca²⁺ exchange) to the outward currents. In one series of experiments, a K⁺-rich pipette solution containing 20 mM Na⁺ was produced by equimolar replacement of KOH with NaOH. K⁺-free pipette solutions were produced by equimolar replacement of KOH and KCl in the above recipe with Cs⁺ or Li⁺ salts. A K⁺-rich pipette solution containing the voltage-gated K⁺ channel blocker TEA (20 mM) was produced by equimolar replacement of KOH with TEOH. In some experiments, a virtually Ca²⁺-free pipette solution was used in which EGTA was replaced with equimolar BAPTA and no CaCl₂ was added. In other experiments, GTP in the pipette solution was replaced with 1 mM GDPβS. In our experience, removal of ATP from the pipette solution often leads to the activation of the ATP-sensitive K⁺ channel current I_{KATP}. Because I_{KATP} is large (>30 pA/pF), activation of this current may mask the effects of PE on other currents. Thus, it was not possible to test the sensitivity of the PE-sensitive current to intracellular ATP. Experiments on the L-type Ca²⁺ current (I_{Ca,L}) were carried out using the Cs⁺-rich pipette solution and by omitting nifedipine and atenolol from the superfusate.

Whole-cell currents recorded by EPC-9 (HEKA GmbH, Germany) or Axopatch 200B (Axon Instruments, Inc., Union City, CA) patch clamp amplifiers were recorded to the hard drive of a PC using Pulse software (version 8.11; HEKA GmbH, Germany). Whereas the EPC-9 amplifier had a built-in A/D converter, currents recorded using the Axopatch 200B were acquired using an ITC-16 A/D converter (InstruTECH Inc., Port Washington, NY). The sampling rate was typically 2 kHz. Junction potentials and capacitance transients were compensated electronically. Currents were normalized to capacitance as a measure of cell size. Arrows in figures presenting current traces indicate zero current level.

Analysis of Current Inactivation. The effect on peak and late outward currents of varying conditioning potential (CP) for 1 s before depolarization to +40 mV was examined. The dependence of the peak currents on CP from voltages of -80 to +5 mV (V_{CP}) were fitted with single or double Boltzmann equations, respectively, by nonlinear least-squares using IgorPro 3.16B software (Wavemetrics Inc., Lake Oswego, OR) as follows.

$$I_{pk}(V_{CP}) = I_t(1 + \exp((V_{CP} - V_{0.5})/V_{s,1})) + I_{ss} \quad (1)$$

$$I_{pk}(V_{CP}) = I_{t01}/(1 + \exp((V_{CP} - V_{0.5,1})/V_{s,1})) + I_{Kx}/(1 + \exp((V_{CP} - V_{0.5,2})/V_{s,2})) + I_{ss} \quad (2)$$

where V_{0.5}, V_{0.5,1}, and V_{0.5,2} represent the half-maximal voltage of inactivation, V_s, V_{s,1}, and V_{s,2} are the slope of the relation, I_t is the total inactivating current when data are fitted by a single Boltzmann, I_{t01} is the current inactivating at more negative potentials when the data are fitted by a double Boltzmann, I_{Kx} is the current inactivating at less negative potentials when the data are fitted by a double Boltzmann, and I_{ss} is the noninactivating steady-state outward current (Himmel et al., 1999). Note the difference in the definition of I_t and I_{t01} between the two equations.

The time course of inactivation of outward currents were fitted

with single or double exponential equations, respectively, by nonlinear least-squares using IgorPro 3.16B software as follows:

$$I(t) = A_0 + A_1 \times \exp(-t/\tau) \quad (3)$$

$$I(t) = A_0 + A_1 \times \exp(-t/\tau_1) + A_2 \times \exp(-t/\tau_2) \quad (4)$$

where A₀ is the time-independent current, τ₁ and τ₂ are the rapid and slow time constants of inactivation, and A₁ and A₂ are the maximal amplitudes of the rapidly and slowly inactivating currents, respectively. In some cases, the amplitude of the inactivating component of the outward currents was reported as the sum of the A₁ and A₂ components. Where the data were fitted by a single exponential component, A₂ was taken to be 0, and the reported value therefore represents the A₁ component alone.

Analysis of the Concentration-Dependence of 4-Aminopyridine Action. The effect of 4-aminopyridine on the time-independent A₀ component was expressed as a percentage reduction from control.

$$\% \text{reduction} = ((A_{0,\text{control}} - A_{0,4\text{-AP}})/A_{0,\text{control}}) \times 100 \quad (5)$$

where A_{0,control} represents the control value, and A_{0,4-AP} represents the value of A₀ in the presence of 4-AP. The concentration dependence of 4-AP action was fitted by a logistic equation as follows.

$$\% \text{reduction} = \% \text{reduction}_{\text{max}} / (1 + (IC_{50}/[4\text{-AP}])^{n_H}) \quad (6)$$

where % reduction_{max} is the maximal percentage reduction, IC₅₀ is the concentration at which the current was reduced by 50% of control, and n_H is the Hill coefficient.

Spectral Analysis of Current Variance. The variance of the PE-sensitive currents was calculated from the integral of the spectral density function, as follows (Dempster, 1993; Helliwell and Large, 1998). Outward currents elicited by depolarization to +40 mV were sampled at 2 kHz and passed through an 8-pole Bessel filter with a cut-off frequency (f_B) of 1 kHz. Under our recording conditions, the whole-cell configuration simulates a single-pole filter with a cut-off frequency of

$$f_{RC} = 1/(2\pi R_s C_m) \quad (7)$$

where R_s is series resistance and C_m is membrane capacitance. Therefore, only data from cells with a membrane time constant (τ_m = R_sC_m) < 720 μs were included in the analysis (mean τ_m, 556 ± 41 μs, n = 8). The last 1024 data points (i.e., 512 ms) of recorded currents were used for calculation of the power spectrum. The steady state and inactivating components of the currents were subtracted by fitting a single decaying exponential equation to the time course of inactivation and subtracting the current predicted by the fitted equation from the data trace. A Hanning (cosine) window was applied to the data, and the power spectrum was calculated using the fast Fourier transform function of IgorPro 3.16B, with appropriate rescaling (Dempster, 1993). Each current trace was analyzed in blocks of 256 data points; between three and five current traces were used to calculate an averaged spectrum. Thus, the lowest frequency that could be resolved was 7.8 Hz (i.e., 2 kHz/256) and the highest corresponded to the Nyquist frequency of 1 kHz. However, because the cut-off frequency of the whole cell configuration, f_{RC}, for the eight cells included in the analysis ranged from 250 to 400 Hz (297 ± 22 Hz, n = 8), only data ranging from 7.8 to 400 Hz were included in the analysis (Helliwell and Large, 1998). The spectrum in the presence of PE was assumed to represent background noise, and this was subtracted from the control spectrum obtained before superfusion with PE to obtain the spectrum of the PE-sensitive current. The PE-sensitive spectra were fitted by a single Lorentzian function:

$$S(f) = \frac{S(0)}{1 + (ff_c)^2} \quad (8)$$

where $S(0)$ is a constant with units of A^2s , f represents frequency (Hz), and f_c is the corner frequency (Dempster, 1993). The current variance was calculated from the integral of this function:

$$\sigma^2 = \frac{\pi f_c S(0)}{2} \quad (9)$$

Assuming that the PE-sensitive current represented a single population of K^+ -selective channels gating between a single closed state and open state with an open probability ≤ 0.1 , the single channel conductance was calculated as:

$$\gamma = \frac{\sigma^2}{\Delta I(V_m - E_K)} \quad (10)$$

where ΔI is the portion of the macroscopic steady-state current inhibited by PE, V_m is the pulse potential (i.e., +40 mV), and E_K is the equilibrium potential for K^+ ions in these experiments (~ -95 mV) (Dempster, 1993; Helliwell and Large, 1998).

Statistics. Data are presented as the mean \pm S.E.M. Current-voltage relations were analyzed by two-way analysis of variance. All other results were analyzed by paired or unpaired t tests ($p < 0.05$ were considered significant).

Results

Phenylephrine Inhibits a Time-Independent Outward Current. Using the perforated-patch, whole-cell voltage-clamp technique, membrane depolarization positive to

-50 mV elicited outward currents that activated rapidly to a peak and then partially inactivated over the course of 1s pulses (Fig. 1A). Superfusion with the α_1 -AR agonist PE (10 μ M) reduced the amplitude of the outward currents (Fig. 1A). Current-voltage relations from seven cells in the absence and presence of PE are shown in Fig. 1B. PE significantly reduced both the mean peak and late outward currents from voltages positive to -50 mV (Fig. 1B). PE had no effect on the inward currents negative to -80 mV, indicating that α_1 -ARs did not modulate I_{K1} under these conditions. The reduction of both peak and late outward current is consistent with the inhibition by PE of a time-independent outward current. To substantiate this, outward current from -50 mV and positive was fitted with a double exponential relation, and the conductance of the time-independent component (A_0) was calculated assuming K^+ selectivity. The voltage-dependence of the conductance density from voltages positive to -50 mV is shown in Fig. 1C and clearly demonstrates that PE reduced a time-independent conductance that was independent of voltage over this range of membrane potentials.

To investigate the nature of the PE-sensitive current further, the dependence of outward current on conditioning potential (CP) was examined (Fig. 2A). For each of seven cells, the current evoked on depolarization to +40 mV was plotted against the preceding CP both under control conditions and in the presence of 10 μ M PE; an example is shown

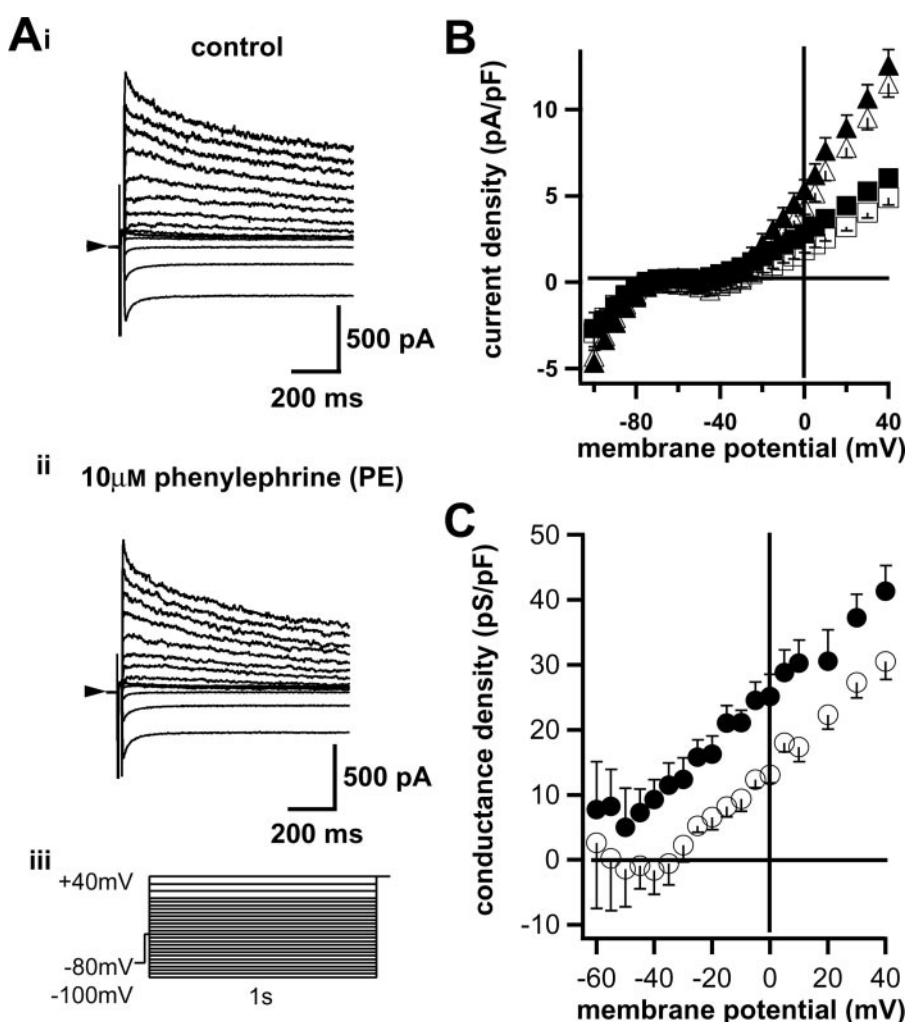


Fig. 1. Phenylephrine inhibits a background current. **A**, representative whole cell current traces recorded using the perforated-patch technique from a rat ventricular myocyte in the absence (i) and presence (ii) of 10 μ M PE using the pulse protocol shown bottom (iii). Holding potential was -80 mV. **B**, current density-voltage relations measured at the peak (triangles) and at the end of the pulse (late current; squares) in the absence (filled symbols) and presence (open symbols) of PE. Data are the mean \pm S.E.M. of seven cells. Peak and late current-voltage relations in the presence of PE were significantly different from control ($p < 0.05$; two-way ANOVA). **C**, conductance density-voltage relations for the time-independent (A_0) component of a double exponential relation fitted to the time course of inactivation of the currents in the absence (●) and presence (○) of PE, calculated assuming a K^+ -selective conductance. Data are the mean \pm S.E.M. from seven cells. Conductance density-voltage relations in the presence of PE were significantly different from control ($p < 0.05$; two-way ANOVA).

in Fig. 2B. The peak outward current showed marked voltage-dependent inactivation, but significant current remained even from depolarized CP, suggesting the existence of inactivating transient (I_t) and noninactivating steady-state (I_{ss}) outward currents in these cells (Fig. 2B). The mean \pm S.E.M. of fitted parameters from a single Boltzmann equation for the seven cells are shown in Table 1. It is clear that the predominant and most significant effect of PE was inhibition of I_{ss} , with no significant effect on I_t under these conditions (Table 1). It is worth noting that in four of the seven cells, including the example shown in Fig. 2, A and B, the voltage-dependent inactivation of the currents could be fitted by a double Boltzmann equation (mean $V_{0.5,1}$ for $I_{t01} = -50.6 \pm 1.9$ mV, mean $V_{0.5,2}$ for $I_{Kx} = -18.9 \pm 3.1$ mV). In these cells, in addition to inhibition of I_{ss} (from 6.92 ± 1.21 pA/pF to 5.41 ± 0.97 pA/pF, $P < 0.02$, $n = 4$), PE inhibited I_{t01} from 12.60 ± 2.12 pA/pF to 7.39 ± 0.85 pA/pF ($P < 0.05$). In contrast, the amplitude of I_{Kx} was slightly, but not significantly, increased by PE (from 2.52 ± 0.68 to 3.75 ± 1.32 pA/pF, $p < 0.09$, $n = 4$). On the other hand, PE did not significantly affect the parameters of voltage-dependent inactivation of I_{t01} or I_{Kx} .

The time course of inactivation of the currents activated on depolarization to +40 mV from a CP of -70 mV (1s) was fitted by a double exponential equation (Fig. 2A). PE affected neither the time constants of inactivation nor the amplitude of the inactivating current components, A_1 and A_2 . Figure 2C shows the mean amplitudes of the inactivating current (cal-

culated as $A_1 + A_2$) and the time-independent current (A_0). It was clear that PE had no effect on the total inactivating current, but it markedly inhibited the time-independent current A_0 (Fig. 2C). Consistent with the voltage-dependent inactivation of I_t (Fig. 2B and Table 1), from a CP of 0 mV the amplitude of the inactivating current was considerably reduced compared with that from a CP of -70 mV, and the time course of inactivation was fitted by a single exponential equation (Fig. 2, A and C). Again, PE significantly inhibited the time-independent current but had no effect on the inactivating current (Fig. 2C). Most significantly, the PE-sensitive current, calculated as the difference between the A_0 component before and during superfusion with PE, was independent of the conditioning potential (CP = -70 mV; 1.69 ± 0.39 pA/pF; CP = 0 mV; 1.75 ± 0.69 pA/pF, $n = 7$). Taken together, these results indicate that PE inhibited a steady-state outward current.

The PE-Sensitive Current Is a K⁺-Selective, Time-Independent Current. The properties of the PE-sensitive current were investigated in detail using conventional whole-cell, voltage-clamp recording. PE (10 μ M) did not alter the inactivating components of the current, but markedly reduced the time-independent A_0 component by 2.32 ± 0.25 pA/pF ($n = 44$; $p < 0.0001$ paired t test, Fig. 3A). PE reduced the amplitude of outward currents measured at the end of 500-ms pulses to +40 mV by 2.26 ± 0.23 pA/pF ($n = 44$); the effect reached a steady state within 4 min (Fig. 3B). The close

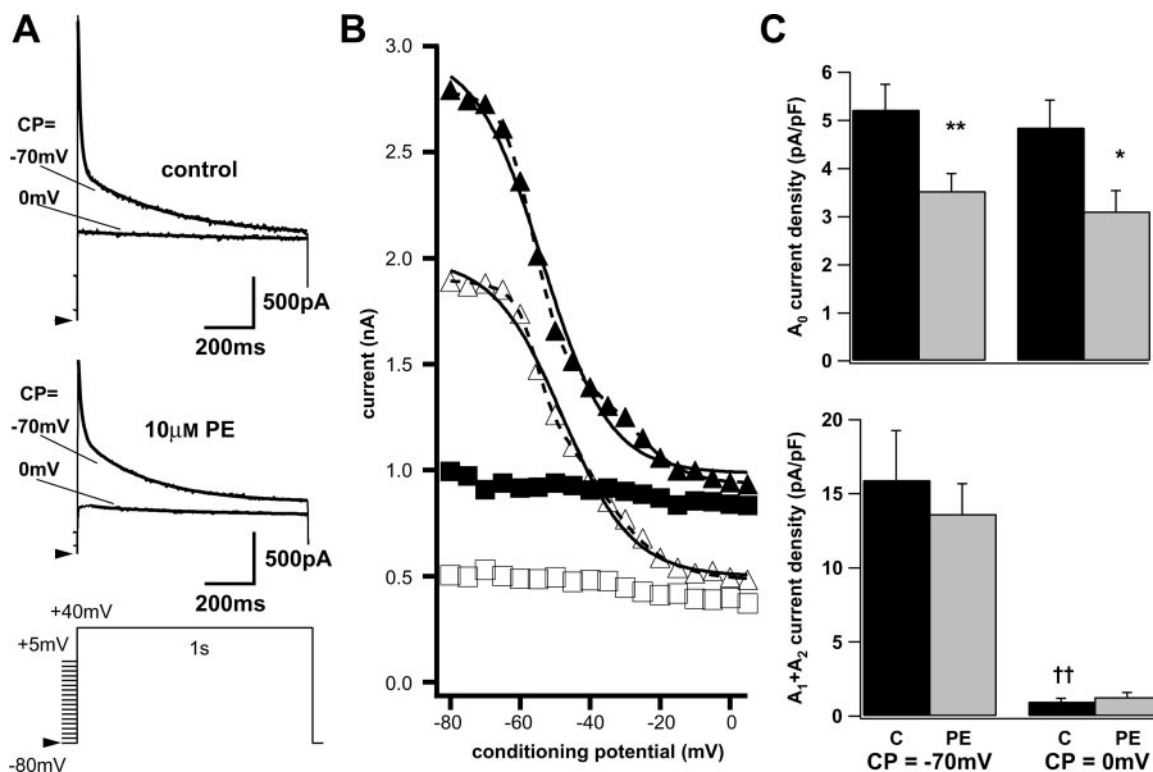


Fig. 2. Phenylephrine inhibits a steady-state outward current. A, representative whole-cell current traces from differing CPs recorded using the perforated-patch technique from a rat ventricular myocyte in the absence (top) and presence (middle) of 10 μ M PE using the pulse protocol shown (bottom). Solid lines represent fits to a single exponential (CP = 0 mV; eq. 3) and a double exponential (CP = -70 mV; eq. 4). Holding potential was -80 mV. B, the effect of CP on steady-state inactivation of peak (triangles) and late (squares) currents in the absence (filled symbols) and presence (open symbols) of PE for the cell shown in A. The solid lines represent fits to a single Boltzmann (eq. 1). The $V_{0.5}$ for I_t under control conditions for the data shown was -53.6 mV. The dashed lines represent fits to a double Boltzmann (eq. 2). The $V_{0.5}$ for I_{t01} and I_{Kx} under control conditions for the data shown were -56.3 and -27.2 mV, respectively. C, the effect of CP potential on the mean \pm S.E.M. of A_0 (top) and $A_1 + A_2$ (bottom) currents in the absence (solid bars) and presence (hatched bars) of 10 μ M PE. *, $p < 0.05$, paired t test versus control from a CP of 0 mV; **, $p < 0.01$, paired t test versus control from a CP of -70 mV; ††, $p < 0.01$, paired t test versus inactivating current from a CP of -70 mV.

correspondence between this value and the PE-sensitive current measured as the A_0 component (2.32 pA/pF) confirms that the predominant current modulated by PE in these cells was a time-independent current. Indeed, subtraction of the currents in the presence of PE from the control currents revealed the time-independent nature of the PE-sensitive current (Fig. 3A). Replacement of pipette K^+ with the monovalent cations Cs^+ or Li^+ markedly reduced the outward currents (Fig. 3, compare C and D with A; note the difference in scale) and effectively abolished the response to PE (Fig. 3E). Thus, PE inhibited a time-independent K^+ -selective outward current.

The Effect of Internal TEA on the PE-Sensitive Current. Many K_v channels are blocked at the internal mouth of the pore by the voltage-gated K^+ channel blocker TEA (Snyders, 1999). To characterize the outward currents further, the effects were investigated of incorporation of TEA (20 mM) in the pipette solution on the currents elicited from CP of -70 and 0 mV (Figs. 4, A and B). Although internal TEA considerably reduced the inactivating ($A_1 + A_2$) currents activated from a CP of -70 mV, there was no effect on the time-independent A_0 (Fig. 4C). From a CP of 0 mV, the $A_1 + A_2$ currents were largely inactivated, and internal TEA had no effect on either the residual inactivating or time-independent currents (Fig. 4D), demonstrating that internal TEA blocked I_t selectively with no effect on I_{ss} . Moreover, even in the presence of internal TEA, PE markedly inhibited A_0 (Fig. 4E) such that the PE-sensitive current was unaffected by internal TEA (Fig. 4F). Therefore, internal TEA differentiated between PE-sensitive and time-dependent current components.

The Effects of External Acidosis and TASK Channel Blockers on the Outward Currents. The effect on the PE-sensitive current of short-term reduction of extracellular pH from 7.35 to 6.1 was determined. Cells were superfused with low pH for 90 to 100 s before administration of $10 \mu M$ PE. Extracellular acidosis differentially affected inactivating and noninactivating currents (Fig. 5, A and B). The amplitude of the inactivating current ($A_1 + A_2$) was markedly increased, whereas A_0 was slightly but not significantly reduced (Fig. 5B). However, the inhibitory effect of PE on the time-independent current (A_0) was almost abolished at low pH (Fig. 5, B and E). TASK-1 K^+ channel currents have been shown to be blocked by the arachidonic acid derivative anandamide, whereas TASK-3 channels are blocked by the cationic dye ruthenium red (Maingret et al., 2001; Czirjak and Enyedi, 2003). Superfusion of myocytes with anandamide ($10 \mu M$) markedly reduced A_0 , with no significant effect on $A_1 + A_2$ (Fig. 5C). Application of PE in the presence of anandamide further decreased A_0 (Fig. 5C). In contrast, ruthenium red ($20 \mu M$) had no significant effect on either A_0 or $A_1 + A_2$ (Fig. 5D). Thus, the PE-sensitive current was partially reduced by

anandamide, whereas ruthenium red had no effect (Fig. 5E). TASK-1 channels have been shown to be blocked by external Zn^{2+} and Ba^{2+} (Duprat et al., 1997; Kim et al., 1999; Leonoudakis et al., 1998). Superfusion with 1 mM $ZnCl_2$ significantly inhibited the A_0 component and increased the amplitude of the $A_1 + A_2$ component, although the latter effect did not reach statistical significance (Fig. 6A; $p = 0.053$, $n = 9$). However, Zn^{2+} did not affect the PE-sensitive current (Fig. 6C). In contrast, 10 mM $BaCl_2$ strongly inhibited both the A_0

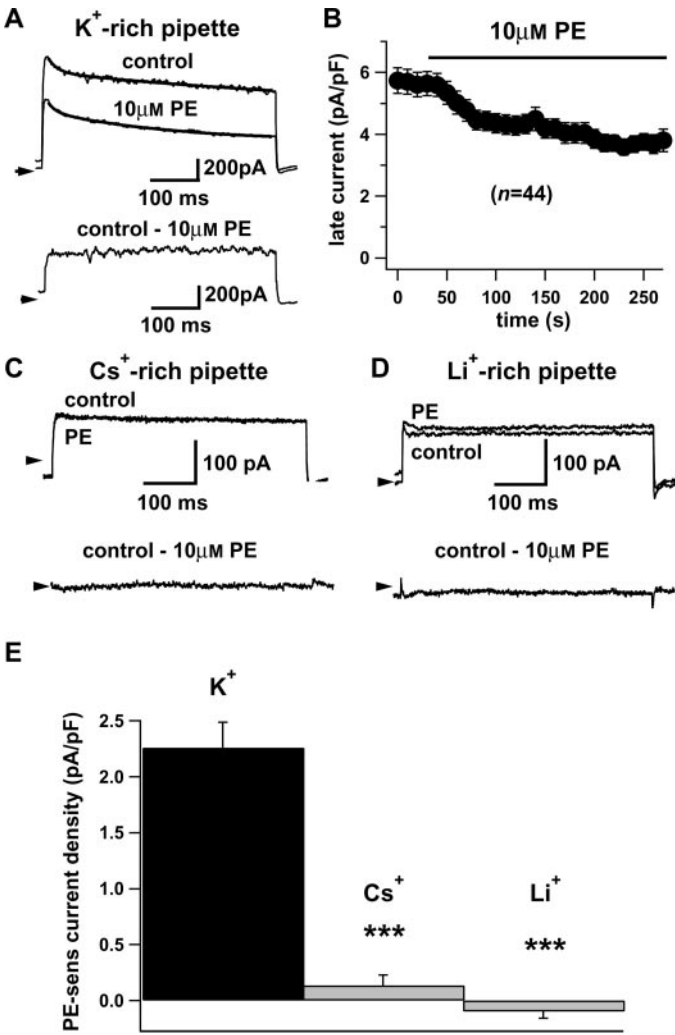


Fig. 3. PE-sensitive current is K^+ -selective. A, top shows example current traces recorded using the conventional whole-cell configuration in the absence and presence of PE using a K^+ -rich pipette solution. Solid lines represent fits to a double exponential relation (eq. 4). In control, $\tau_1 = 17 \pm 2$ ms and $\tau_2 = 294 \pm 26$ ms ($n = 44$). PE had no significant effect on the τ values. Bottom shows the PE-sensitive difference current obtained by subtracting the current in the presence of PE from the control current. B, time course of inhibition of outward current by $10 \mu M$ PE. Currents were recorded using a K^+ -rich pipette solution and measured at the end of pulses to $+40$ mV (500 ms). Holding potential (V_{hold}) was -70 mV. Data are the mean \pm S.E.M. from 44 cells. C, top, example current traces recorded using the Cs^+ -rich pipette solution. Current traces in the presence of PE almost completely overlaid control traces. Note the expanded current scale compared with traces shown in A. Bottom, PE-sensitive difference current. D, top, example current traces recorded using the Li^+ -rich pipette solution. Bottom, PE-sensitive difference current. E, mean \pm S.E.M. of PE-sensitive difference currents measured at the end of pulses to $+40$ mV using K^+ -rich ($n = 44$), Cs^+ -rich ($n = 6$), and Li^+ -rich ($n = 6$) pipette solutions. ***, $p < 0.001$, unpaired t test versus PE-sensitive difference current with a K^+ -rich pipette solution.

TABLE 1
Fitted parameters from seven cells of voltage-dependent inactivation according to a single Boltzmann equation
Data are presented as mean \pm S.E.M.

Parameter	Control	$10 \mu M$ PE	P
I_t	11.11 ± 2.50 pA/pF	9.04 ± 1.31 pA/pF	N.S.
$V_{0.5}$	-45.9 ± 3.1 mV	-43.4 ± 0.31 mV	N.S.
V_s	7.5 ± 0.8 mV	9.6 ± 0.9 mV	N.S.
I_{ss}	6.10 ± 0.50 pA/pF	4.45 ± 0.31 pA/pF	$P < 0.02$

and A₁ + A₂ components and markedly reduced the PE-sensitive current (Fig. 6, B and C).

The Effect of K⁺ Channel Blockers on the PE-Sensitive Current. 4-AP and TEA, applied externally, have been reported to inhibit partially I_{ss} in rat ventricular myocytes (Apkon and Nerbonne, 1991; Himmel et al., 1999). Consistent with these reports, 4-AP was found to inhibit the A₀ component in a concentration-dependent manner, producing a maximal inhibition of ~20% reduction from control at 10 mM (Fig. 7A). In contrast, 10 mM 4-AP reduced the inactivating component (A₁ + A₂) by 82.5 ± 6.1% of control (*n* = 8). Most notably, in the presence of 10 mM 4-AP, the response to 10 μM PE was reduced to approximately 45% of control (Figs. 7B and 7C). 10 mM external TEA also partially inhibited the

time-independent A₀ component (20.3 ± 6.9%, *n* = 6; Fig. 8A). However, in contrast to the action of 4-AP, 10 mM TEA did not significantly affect the inactivating current (Fig. 8A). In the presence of 50 mM external TEA, both the A₀ and the A₁ + A₂ components were markedly reduced from control (Fig. 8B). The PE-sensitive current was significantly reduced in the presence of 10 and 50 mM external TEA (Fig. 8C).

The Effect of PE on the Power Spectrum of Current Noise. During the course of these experiments, it was noted that the noise of outward whole-cell currents was generally reduced in the presence of 10 μM PE (Fig. 9A). Because it was conceivable that the inhibitory effect of PE on the whole-cell currents might be associated with the inhibition of activity of K⁺ channels of relatively large unitary conductance, a spec-

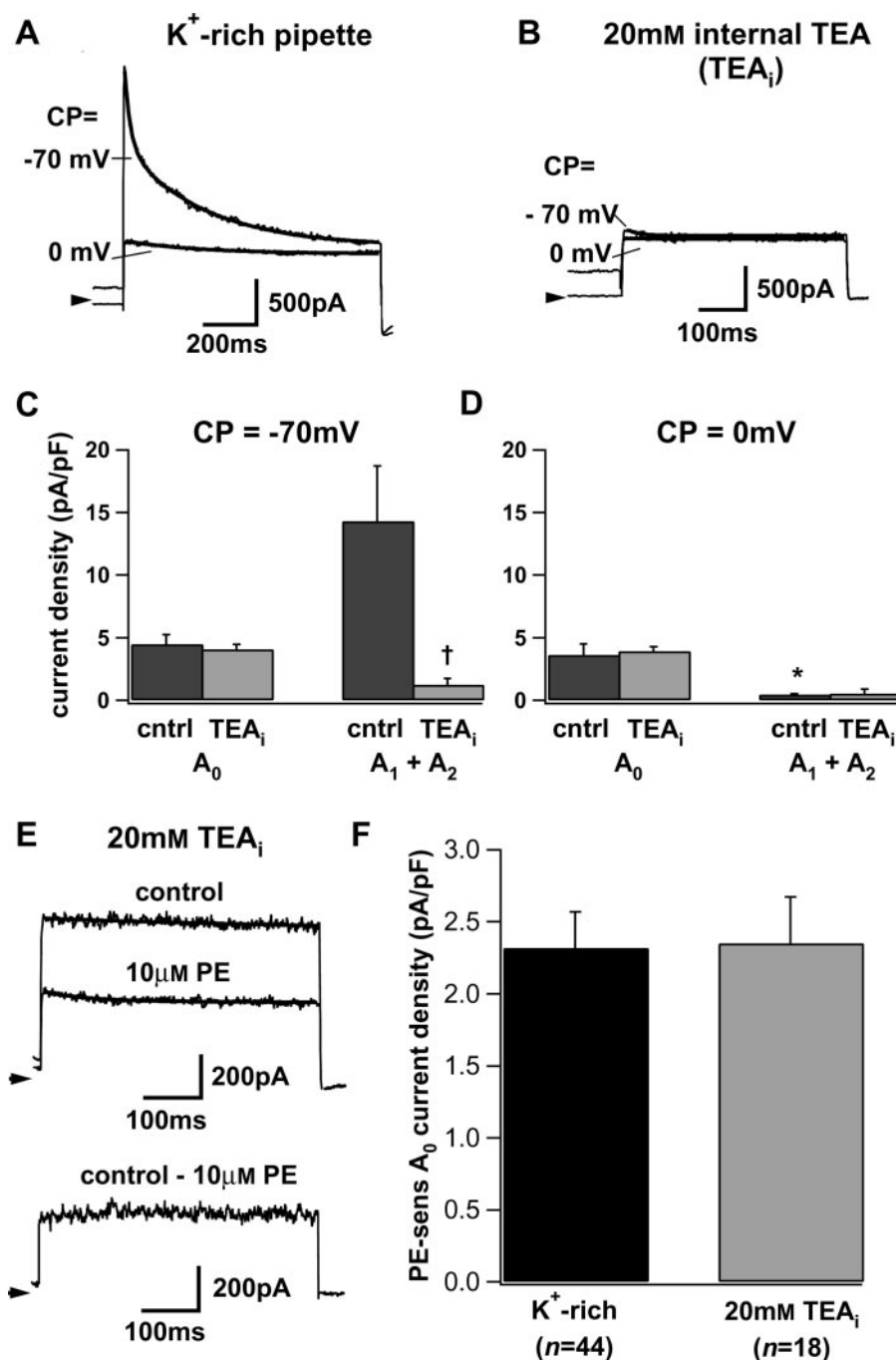


Fig. 4. Phenylephrine-sensitive current is not blocked by intracellular TEA. A, example current traces from CPs of -70 and 0 mV recorded using the conventional whole-cell configuration and a K⁺-rich pipette solution. Solid lines represent fits to double (CP = -70 mV) or single (CP = 0 mV) exponential equations. B, example current traces from CPs of -70 and 0 mV recorded using the conventional whole-cell configuration and a pipette solution containing 20 mM TEA. Solid lines represent fits to double (CP = -70 mV, eq. 4), or single (CP = 0 mV, eq. 3) exponential relations. C, effect of internal TEA (TEA_i) on time-independent (A₀) and inactivating (A₁ + A₂) components from a CP of -70 mV. Data are the mean ± S.E.M. of seven cells. †, *p* < 0.05, unpaired *t* test versus inactivating current from CP = -70 mV recorded using a K⁺-rich pipette solution. D, effect of TEA_i on time-independent (A₀) and inactivating (A₁ + A₂) components from a CP of 0 mV. Data are the mean ± S.E.M. of seven cells. *, *p* < 0.05, paired *t* test versus inactivating current from CP = -70 mV recorded using a K⁺-rich pipette solution. E, top, example current traces recorded using the conventional whole-cell configuration in the absence and presence of PE using a pipette solution containing TEA. Solid lines represent a fit to a single exponential relation (eq. 3). Bottom shows the PE-sensitive current obtained by subtracting the current in the presence of PE from the control current. F, mean PE-sensitive difference currents calculated by subtracting the A₀ component in the presence of PE from the control. Data represent mean ± S.E.M.; numbers in brackets indicate sample sizes. Note that although intracellular TEA markedly inhibited the inactivating current (compare B with A), it had no effect on the PE-sensitive current.

tral analysis of the current noise was conducted on eight cells that fell within our exclusion criterion (see *Materials and Methods*). Figure 9B shows the power spectra for the currents shown in Fig. 9A in the absence and presence of 10 μ M PE. As expected from visual inspection of the current traces (e.g., Fig. 9A), the power of the noise at frequencies of 7.8 Hz and above was consistently reduced in the presence of PE (Fig. 9B). The power spectrum in the presence of PE was assumed to represent background noise and was subtracted from the control power spectrum to give the power spectrum of the

PE-sensitive current. The power spectrum of the PE-sensitive current was fitted with a single Lorentzian (eq. 8 with mean $S(0) = 25.4 \pm 9.2$ pA²s and mean $f_c = 116 \pm 20$ Hz ($n = 8$). If the PE-sensitive current represented a single population of K⁺-selective channels, the mean single channel conductance (γ) calculated according to eq. 10 was 77.9 ± 4.3 pS ($n = 8$). We were concerned that with the exclusion criteria used, the attenuation of the power spectrum at frequencies above the cut-off frequency, f_{RC} , might lead to error in the estimation of the single-channel conductance. However, if this were the case, it might be expected that there should be a correlation between the value of f_{RC} and the single channel

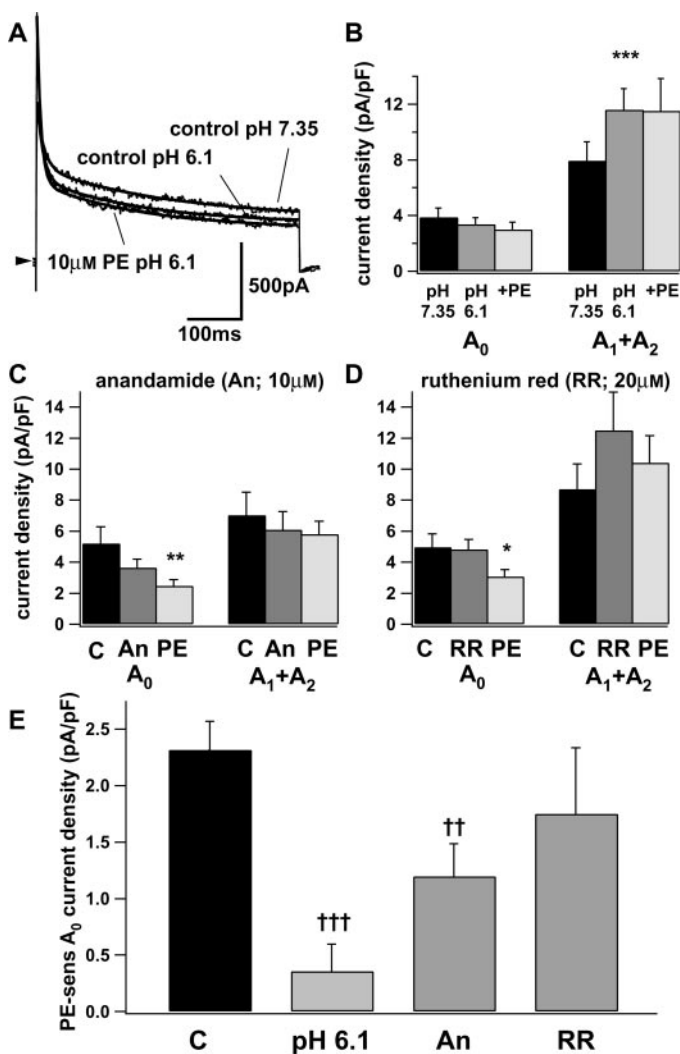


Fig. 5. Effect on PE-sensitive current of external acidosis and acid-sensitive K⁺ channel blockers. **A**, example current traces recorded on depolarization to +40 mV at control pH (pH 7.35), at acid pH (pH 6.1), and in the presence of 10 μ M PE at acid pH. Holding potential was -70 mV. Solid lines represent fits to a double exponential relation (eq. 4). **B**, mean A_0 and $A_1 + A_2$ components from seven cells in which external pH was lowered to 6.1. ***, $p < 0.001$ paired t test compared with $A_1 + A_2$ at pH 7.35. **C**, mean A_0 and $A_1 + A_2$ components from seven cells superfused with 10 μ M anandamide. **, $p < 0.01$ paired t test compared with A_0 in the presence of anandamide alone. **D**, mean A_0 and $A_1 + A_2$ components from six cells superfused with 20 μ M ruthenium red. *, $p < 0.05$ paired t test compared with A_0 in the presence of ruthenium red alone. **E**, mean \pm S.E.M. of PE-sensitive difference currents calculated by subtracting the A_0 component in the presence of PE from the control under control conditions (C, $n = 44$), at an external pH of 6.1 ($n = 7$), in the presence of anandamide (An, $n = 7$), and in the presence of ruthenium red (RR, $n = 6$). †††, $p < 0.001$, unpaired t test versus PE-sensitive difference current under control conditions; ††, $p < 0.01$, unpaired t test versus PE-sensitive difference current under control conditions.

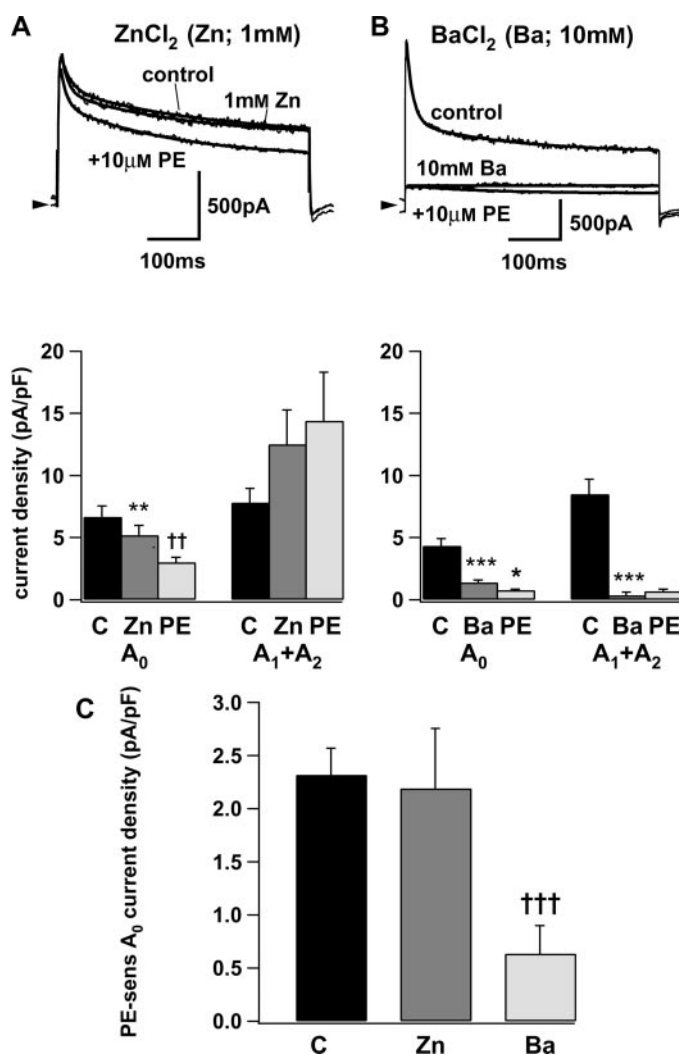


Fig. 6. Effect on PE-sensitive current of divalent cations. **A**, top, example current traces under control conditions, in the presence of 1 mM ZnCl₂ and in the presence of 1 mM ZnCl₂ plus 10 μ M PE. Solid lines represent fits to a double exponential relation (eq. 4). Lower shows the mean \pm S.E.M. of the time-independent (A_0) and inactivating ($A_1 + A_2$) currents for nine cells exposed to 1 mM ZnCl₂. **, $p < 0.01$, paired t test compared with control; ††, $p < 0.01$, paired t test versus A_0 in the presence of ZnCl₂. **B**, top shows example current traces under control conditions, in the presence of 10 mM BaCl₂ and in the presence of 10 mM BaCl₂ plus 10 μ M PE. Solid lines represent fits to a double exponential relation (eq. 4). Lower shows the mean \pm S.E.M. of the time-independent (A_0) and inactivating ($A_1 + A_2$) currents for eight cells exposed to 10 mM BaCl₂. ***, $p < 0.001$, paired t test versus control; *, $p < 0.05$, paired t test versus A_0 in the presence of BaCl₂. **C**, PE-sensitive difference in A_0 currents in control cells ($n = 44$), in the presence of 1 mM ZnCl₂ ($n = 9$) and 10 mM BaCl₂ ($n = 8$). †††, $p < 0.001$, unpaired t test versus control.

conductance. No such relation existed. Thus, the above estimate of single channel conductance was not different from that obtained using three of these cells that fulfilled more stringent exclusion criteria ($\tau_m < 500 \mu\text{s}$, f_{RC} ranging from 345 to 400 Hz) in which mean $S(0) = 14.7 \pm 6.1 \text{ pA}^2\text{s}$, mean $f_c = 140 \pm 10 \text{ Hz}$, corresponding to a mean single-channel conductance of $75.8 \pm 5.9 \text{ pS}$.

The Effect of Quinidine on the PE-Sensitive Current: Evidence for Involvement of Slick. The high unitary conductance of the PE-sensitive current (Fig. 9) and its partial sensitivity to external 4-AP (Fig. 7) and TEA (Fig. 8) are reminiscent of Slick voltage-gated K⁺ channels (Bhattacharjee et al., 2003). Because Slick channels are blocked by external administration of high concentrations of quinidine, the effect on the PE-sensitive current of this antiarrhythmic drug was examined (Fig. 10). Quinidine (100 μM) inhibited the time-dependent $A_1 + A_2$ component by $70.7 \pm 12.4\%$ and the time-independent A_0 component by $58.4 \pm 3.4\%$ ($n = 6$, Fig. 10, A and B). Moreover, in the presence of 100 μM quinidine, the PE-sensitive time-independent current was markedly and significantly reduced (Fig. 10C). The inhibitory response to PE was effectively abolished by 1 mM quinidine, although there was also evidence of nonspecific actions on the whole-cell membrane current at this very high concentration ($n = 5$, data not shown).

Slick channel activity is reported to be increased by very high concentrations of Na⁺ (i.e., $> 20 \text{ mM}$; $\text{EC}_{50} = 81 \text{ mM}$, $n_H = 1.4$) at the cytosolic surface of excised membrane patches from Chinese hamster ovary cells transfected with the Slick cDNA (Bhattacharjee et al., 2003). No information is available regarding the Na⁺ sensitivity of native Slick channels (either from excised patches or whole-cell recordings) from any cell type. Estimates of intracellular [Na⁺] in rat ventricular myocytes range from 10 to 20 mM, depending on the recording conditions and stimulation frequency (Despa et al., 2002). Therefore, the effect on the PE-sensitive current of dialyzing the cells with a pipette solution containing a concentration of Na⁺ at the upper end of the physiological range was investigated. However, the amplitude of the PE-sensi-

tive current recorded with a pipette [Na⁺] = 20 mM ($1.75 \pm 0.47 \text{ pA/pF}$, $n = 7$) was not significantly different from that recorded under control conditions. Thus, the PE-sensitive current was insensitive to intracellular Na⁺ in the physiological concentration range. Because the sensitivity of Slick channels in excised inside-out patches to Na⁺ at the cytosolic surface of the patch operates predominantly in a supraphysiological range of concentrations, this observation does not preclude the involvement of Slick channels to the PE-sensitive current.

The Involvement of α_1 -ARs in Current Modulation. The response to PE was effectively abolished in the presence of the α_1 -AR antagonist, prazosin (1 μM , Fig. 11A). However, pretreatment of the cells with the site-specific alkylating reagent CEC, which modifies α_{1B} - and α_{1D} - but not α_{1A} -ARs (Zhong and Minneman, 1999), did not attenuate the response to PE (Fig. 11, A and B). Indeed, PE produced an effect in CEC-pretreated cells similar to that observed in control cells (compare Figs. 11B and 3A). The α_{1A} -AR-specific antagonist WB4101 almost completely abolished the response to PE, in a manner similar to that of prazosin (Fig. 11A), suggesting that the response to PE was mediated predominantly by α_{1A} -ARs. Furthermore, the α_{1A} -specific agonist A61603 inhibited a time-independent current in a manner similar to PE (Fig. 11, A and C).

Investigation of the Signaling Pathways Involved in the PE-Response. α_1 -Adrenoceptors activate multiple intracellular signaling pathways, principally involving G_q GTP-binding proteins, although they have also been reported to couple to pertussis toxin (PTX)-sensitive G-proteins (Fedida et al., 1993a; Zhong and Minneman, 1999). The response to PE was considerably reduced in cells in which intracellular GTP was depleted by including GDP β S in the pipette solution (Fig. 12A). On the other hand, the response to PE was not reduced by preincubation of cells with PTX for at least 1 h at 37°C (Fig. 12A). The inhibition of G_{i/o}-mediated pathways in the PTX-treated cells was confirmed by examining the action of the muscarinic agonist carbachol on $I_{Ca,L}$ in the presence of the β -AR agonist isoprenaline (data not shown).

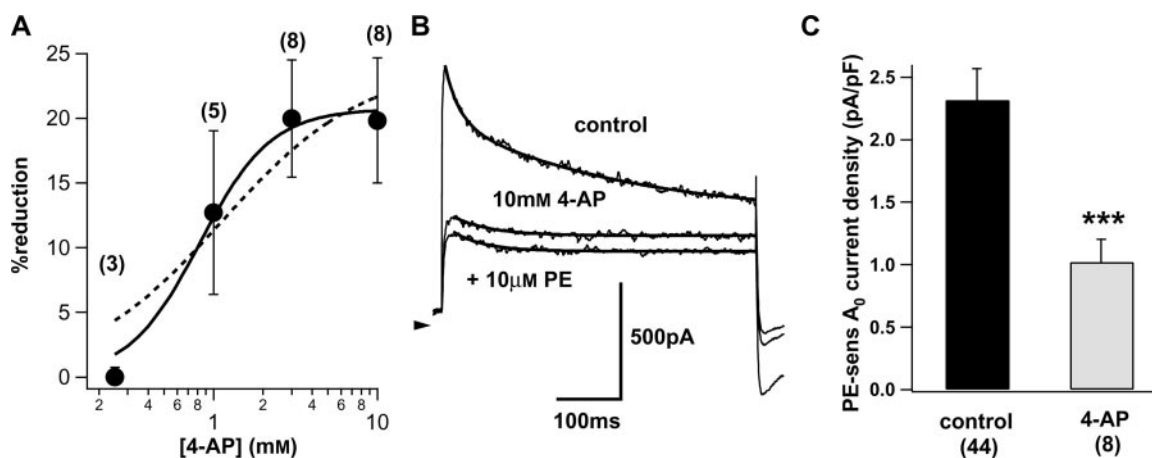


Fig. 7. Effect of external 4-aminopyridine on the PE-sensitive current. A, concentration dependence of the effect of 4-aminopyridine on the time-independent (A_0) current. Numbers in brackets represent cell numbers. Solid line represents a fit to a logistic equation with a Hill coefficient of 2 (eq. 6). The maximal current inhibition was 20.7%, and the IC_{50} was $0.68 \mu\text{M}$. Dotted line represents fit to a logistic equation with a Hill coefficient of 1. B, example current traces under control conditions, in the presence of 10 mM 4-AP and in the presence of 10 mM 4-AP plus 10 μM PE. Solid lines represent fits to a double exponential relation (eq. 4). C, mean \pm S.E.M. of PE-sensitive A_0 difference currents under control conditions ($n = 44$) and in the presence of 10 mM 4-AP ($n = 8$). ***, $p < 0.001$, unpaired t test versus control PE-sensitive A_0 difference current. The PE-sensitive current was also significantly reduced in the presence of 3 mM 4-AP ($1.04 \pm 0.37 \text{ pA/pF}$; $n = 6$). The effect of 3 mM 4-AP was not significantly different from 10 mM 4-AP (unpaired t test).

On the other hand, incorporation in the pipette of the G_q -antagonist peptide GP2A (Mukai et al., 1992) slightly but significantly inhibited the response to PE (Fig. 12A). Strongly buffering intracellular Ca^{2+} using BAPTA had no effect on the PE response (Fig. 12A). In contrast, pretreatment of the cells for 10 min with U73122 (5 μ M), a widely used inhibitor of phospholipase C (PLC), reduced the effect of PE (Fig. 12B). However, this effect of U73122 was not significantly different from that of its inactive analog U73343 (5

μ M). Moreover, the nonselective inhibitor of PLC and phospholipase D, neomycin, had no effect on the responses to PE (Fig. 12B) (Liscovitch et al., 1991). Likewise, although treatment of the cells with 40 μ M AACOCF₃, a phospholipase A₂ (PLA₂) inhibitor, significantly reduced the response to PE, an alternative PLA₂ inhibitor, MAFP (25 μ M), had no effect (Fig. 12B). Interventions targeted at protein kinase C (PKC) did not significantly affect the response to PE (Fig. 12C). Although the response to PE was significantly reduced by the tyrosine kinase inhibitor genistein (50 μ M), the control currents before administration of PE were also reduced. Thus, a nonspecific action of the isoflavone on the steady-state current cannot be ruled out (Fig. 12C). On the other hand, intracellular administration of the phosphatidylinositol 3-kinase (PI 3-kinase) inhibitor wortmannin (5 μ M) significantly reduced the response to PE but not the control current (Fig. 12C).

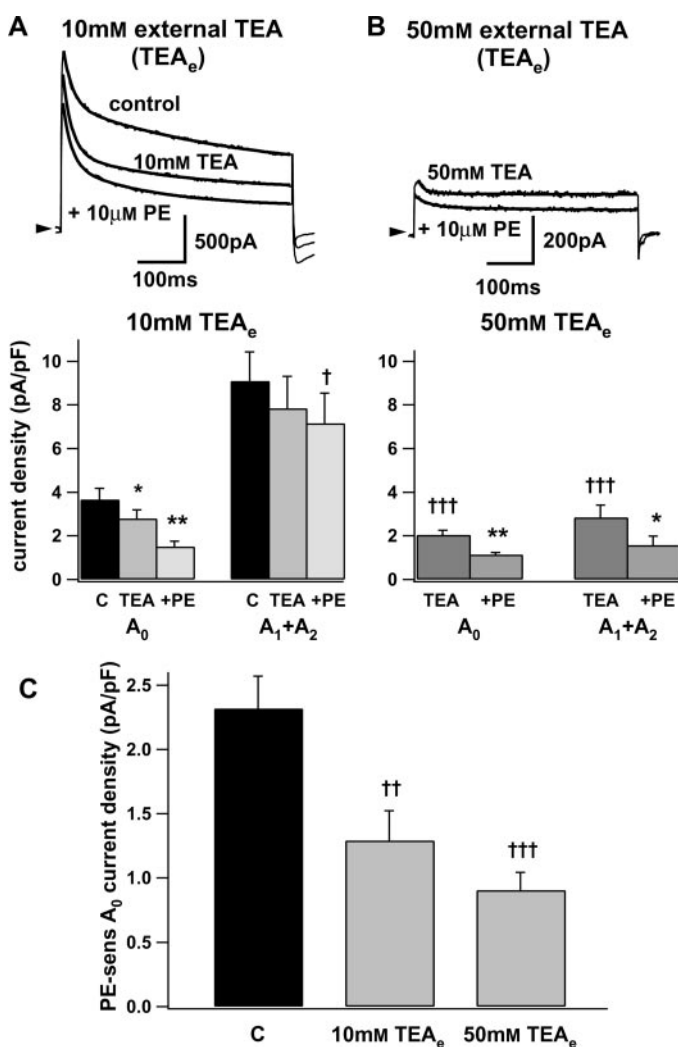


Fig. 8. Effect of external TEA on PE-sensitive current. **A**, top, example current traces under control conditions, in the presence of 10 mM external TEA (TEA_e) and in the presence of 10 mM TEA_e plus 10 μ M PE. Solid lines represent fits to a double exponential relation (eq. 4). Bottom, mean \pm S.E.M. of the time-independent (A_0) and inactivating ($A_1 + A_2$) currents for six cells exposed to 10 mM TEA_e . *, $p < 0.05$, paired t test compared with control; **, $p < 0.01$, paired t test compared with A_0 in the presence of TEA_e ; †, $p < 0.05$, paired t test versus $A_1 + A_2$ current in the presence of 10 mM TEA_e . **B**, top, example current traces in the presence of 50 mM TEA_e and 50 mM TEA_e plus 10 μ M PE. Solid lines represent fits to a double exponential equation. Lower shows the mean \pm S.E.M. of the time-independent (A_0) and inactivating ($A_1 + A_2$) currents for six cells exposed to 50 mM TEA_e . †††, $p < 0.001$, unpaired t test versus corresponding control current densities; **, $p < 0.01$, paired t test versus A_0 in the presence of 50 mM TEA_e ; *, $p < 0.05$, paired t test versus $A_1 + A_2$ current in the presence of 50 mM TEA_e . **C**, mean \pm S.E.M. of PE-sensitive A_0 difference currents under control conditions (C, $n = 44$) and in the presence of 10 mM ($n = 6$) and 50 mM ($n = 6$) TEA_e . ††, $p < 0.01$, unpaired t test versus control PE-sensitive A_0 difference current; †††, $p < 0.001$, unpaired t test versus control PE-sensitive A_0 difference current.

Discussion

This report demonstrates that PE inhibits a K^+ -selective current with properties distinct from other cardiac currents

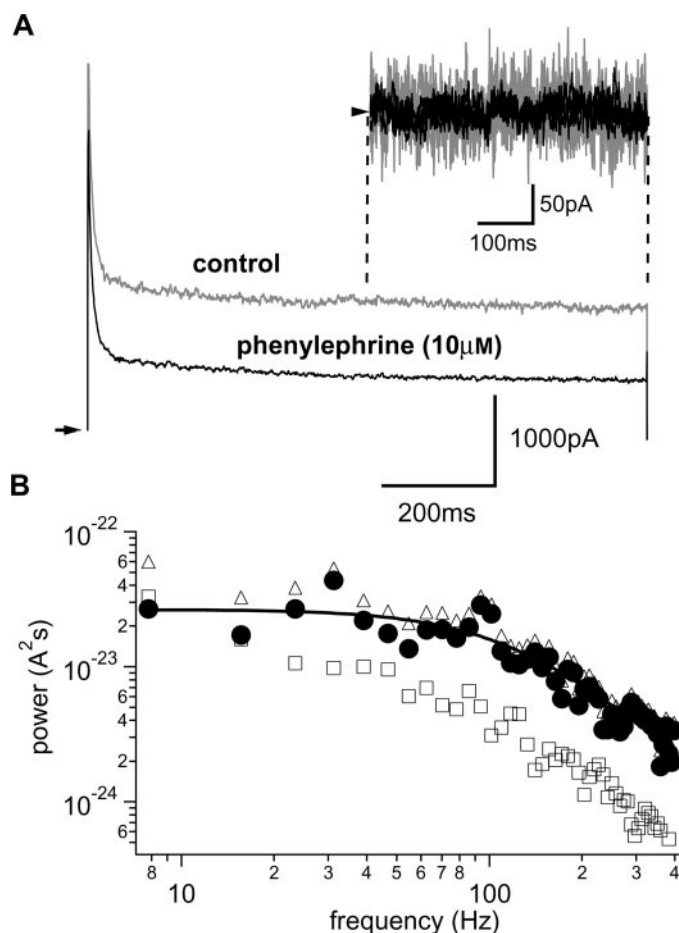


Fig. 9. Spectral analysis of PE-sensitive current. **A**, example current traces under control conditions (gray) and in the presence of 10 μ M PE (black). Inset shows the last 1024 data points of the current traces after subtraction of the steady state and inactivating components. **B**, power spectra of the control current (Δ) and the current in the presence of PE (\square) for the data shown in **A**. ●, power spectrum of the PE-sensitive component calculated by subtracting the background power spectrum from control. The solid line represents a fit to the PE-sensitive power spectrum using eq. 8 ($S(0) = 26.4$ pA²s, $f_c = 124$ Hz). The single channel conductance calculated for this cell using eq. 10, $\gamma = 75.2$ pS.

characterized to date (Snyders, 1999). Moreover, the data show that the inhibitory response to PE was mediated predominantly through α_{1A} -adrenoceptors, via a pathway involving PTX-insensitive G-proteins and PI 3-kinase but independent of cytosolic Ca²⁺ and phospholipase C.

The Predominant Current Modulated by PE Is a K⁺-Selective Steady-State Current. Two lines of evidence demonstrate that the A₀ and the A₁ + A₂ components obtained by curve-fitting represent distinct K⁺ channel types: 1) the A₁ + A₂ components were markedly reduced (~16-fold) by conditioning pulses to 0 mV, whereas the A₀ component was unaffected (Fig. 2, A and C); 2) the A₁ + A₂ currents were effectively (~17-fold) and selectively inhibited by incorporation of the voltage-gated K⁺ channel blocker, TEA, in the

pipette solution (Fig. 4), whereas the PE-sensitive current was insensitive to internal TEA but was K⁺-selective (Fig. 4E). The notion that a steady-state current represents the predominant current modulated by PE was supported by Boltzmann analysis of voltage-dependent inactivation (Fig. 2 and Table 1). These data are consistent with the propositions that: a) the sum of the A₁ and A₂ components represents I_t; b) Kv1.x and Kv4.x channels contribute to I_t in these cells, and c) A₀ represents a steady-state K⁺ current, I_{ss}, distinct from I_t (Himmel et al., 1999; Snyders, 1999).

α_1 -ARs have been reported previously to inhibit cardiac I_{to1} (Fedida et al., 1993a). Considerable heterogeneity exists between cells in the relative contribution of subcomponents of the transient outward current (Himmel et al., 1999; Snyders, 1999), and we do not exclude the possibility that α_1 -ARs are able to modulate I_{to1} under some experimental conditions. For example, in experiments performed using the perforated patch recording technique, the voltage-dependent inactivation of the currents in a subset of the cells could be fitted by a double Boltzmann equation (Fig. 2) according to Himmel et al. (1999). In these four cells, I_{to1} (but not I_{Kx}) was significantly inhibited by PE in addition to I_{ss}. Nevertheless, the predominant effect of PE in experiments performed using either the perforated-patch (*n* = 7; Fig. 2) or conventional whole-cell (*n* = 44; Fig. 3) recording techniques was the inhibition of a time-independent outward current (A₀) with no significant overall effect on the inactivating currents (A₁ + A₂). It is therefore possible to attribute with confidence the observed effects of α_1 -AR activation on A₀ to effects on I_{ss} rather than on I_t.

Properties of the PE-Sensitive Current (I_{ss,PE}). The power spectrum of the PE-sensitive current noise could be fitted by a single Lorentzian component (Fig. 9), an observation consistent with the contribution of a single population of channels to the PE-sensitive current (Dempster, 1993). Assuming a linear open channel current-voltage relation for a single population of K⁺-selective channels, the unitary channel conductance was estimated to be ~78 pS (Fig. 9). However, based on the data shown in Figs. 6 to 10, the possibility that the PE-sensitive current represents a heterogeneous current of more than one population of channels cannot be entirely excluded. Nevertheless, although the unitary conductance would be underestimated in that case, the noise analysis suggests the contribution of a channel of at least 78 pS to the PE-sensitive current. The absence of effect of PE on the inward currents at potentials negative to E_K (Fig. 1B) indicates that the PE-sensitive current shows outward rectification, consistent with the involvement of a voltage-dependent channel. On the other hand, the conductance-voltage relation shows that the PE-sensitive current was fully activated at potentials positive to -50 mV (Fig. 1C). Although no inactivation of I_{ss,PE} could be observed in the present study (Figs. 2 and 3), our data do not exclude the possibility that the PE-sensitive current inactivates very slowly (time constant >1s). In summary, I_{ss,PE} represents a current through a rapidly activating K⁺ channel with unitary conductance of at least 78 pS that produces an outwardly rectifying current that either does not inactivate or inactivates only very slowly.

The lack of inhibition of the PE-sensitive current by internal TEA, which can be expected to block the voltage-gated K⁺ channel α -subunits thought to underlie cardiac I_{Kur} (Fedida

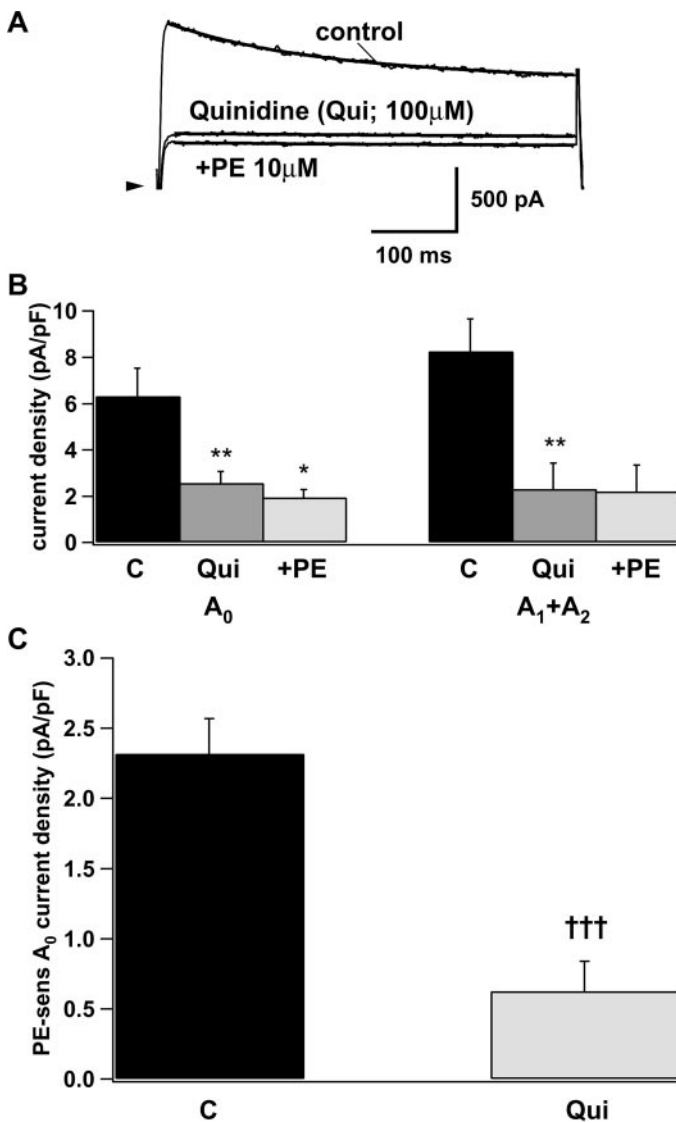


Fig. 10. Effect of quinidine on the PE-sensitive current. A, top, example current traces under control conditions, in the presence of 100 μ M external quinidine (Qui) and in the presence of 100 μ M Qui plus 10 μ M PE. Solid lines represent fits to a double exponential relation (eq. 4). B, left, mean \pm S.E.M. of the time-independent (A₀); right, inactivating (A₁ + A₂) currents for six cells exposed to 100 μ M Qui. *, *p* < 0.05, paired *t* test compared with A₀ in the presence of 100 μ M Qui; **, *p* < 0.01, paired *t* test compared with control. C, mean \pm S.E.M. of PE-sensitive A₀ difference currents under control conditions (C, *n* = 44) and in the presence of 100 μ M Qui (*n* = 6). †††, *p* < 0.001, unpaired *t* test versus control PE-sensitive A₀ difference current.

et al., 1996; Nattel et al., 1999; Shieh and Kirsch, 1994; Taglialatela et al., 1994), is inconsistent with the suggestion (van Wagoner et al., 1996; Nattel et al., 1999) that $I_{ss,PE}$ represents a subtype of I_{Kur} (Fig. 4F). Moreover, both control I_{ss} and the PE-sensitive current were only partially inhibited by relatively high concentrations of 4-AP (Fig. 7), which would be expected to block I_{Kur} completely (Nattel et al., 1999). Furthermore, the unitary conductances reported for the Kv1.5, Kv1.2, Kv2.1, or Kv3.1 I_{Kur} channels (13–25 pS) are much lower than $I_{ss,PE}$ (Fedida et al., 1993b; Shahidullah et al., 1995; Shieh and Kirsch, 1994; Taglialatela et al., 1994). Taken together, our data suggest that the inhibitory response to PE involves a current distinct from I_{Kur} .

Although short-term acidosis reduced the inhibitory response to PE by ~88% (Fig. 5E), the control time-independent current was not significantly reduced by acidosis (Fig. 5B); this finding is inconsistent with the involvement of acid-sensitive K^+ channels in the PE-sensitive current. At concentrations sufficient to produce complete block of TASK-1 channels, anandamide (10 μ M; Maingret et al., 2001) produced only partial inhibition of the PE response, whereas Zn^{2+} (Leonoudakis et al., 1998) was without effect (Figs. 5 and 6). The TASK-3 inhibitor ruthenium red also had no effect (Fig. 5E). Moreover, the biophysical properties of the PE-sensitive current are quite distinct from TASK-1: TASK-1 channels have a unitary conductance of 14 pS (Kim et al., 1999) and produce 'leak' background K^+ currents that pass inward current negative to E_K (Duprat et al., 1997). Thus, taken together, our data do not support a predominant role for TASK channels in the PE response. Three properties of I_{ss} are inconsistent with the involvement of TREK: 1) the inhibitory response to PE was observed in the absence of either membrane stretch or exogenous polyunsaturated fatty acids;

2) TREK is insensitive to external TEA; 3) TREK-1 has a unitary conductance of 48 pS in physiological external $[K^+]$ (Patel et al., 1998).

Slick—A Possible Molecular Basis to $I_{ss,PE}$? Slick is a very recently identified slo-type voltage-gated K^+ channel that is expressed in the heart (Bhattacharjee et al., 2003). However, no native Slick-like cardiac current has yet been identified. The PE-sensitive current characterized in this study resembles Slick K^+ channel currents with respect to large unitary conductance (Fig. 9), outward rectification (Fig. 1C), maximal activation at potentials positive to -50 mV (Fig. 1C), time-independence (Fig. 3), partial sensitivity to high concentrations of external TEA (Fig. 8), and sensitivity to external Ba^{2+} and quinidine (Figs. 6 and 10) (Bhattacharjee et al., 2003). Moreover, slo channels are relatively insensitive to blockade by internal TEA (Moss and Magleby, 2001). These similarities suggest that further work is now required to establish the contribution of Slick to $I_{ss,PE}$.

PE Acts Predominantly via α_{1A} -ARs Acting through a PTX-Insensitive G-Protein. The effect of prazosin on the response to PE confirms the involvement of α_1 -adrenoceptors in modulation of I_{ss} (Fig. 11A). The lack of effect on the responses to PE of pretreatment with α_{1B} - and α_{1D} -AR-selective inhibitor and the marked inhibition by the α_{1A} -AR-selective antagonist, WB4101 suggest that the responses to PE were predominantly mediated via the α_{1A} -AR (Fig. 11, A and B). This conclusion is supported by the inhibitory effect of the α_{1A} -AR agonist A61603 on I_{ss} (Fig. 11, A and C). The marked attenuation of the PE-sensitive current in GDP β S-dialyzed cells and the lack of effect of PTX demonstrated the involvement of PTX-insensitive G-proteins, presumably G_q , in the response to the α_1 -agonist (Fig. 12A). The inhibitory effect of the antagonist peptide GP2A on the response to PE

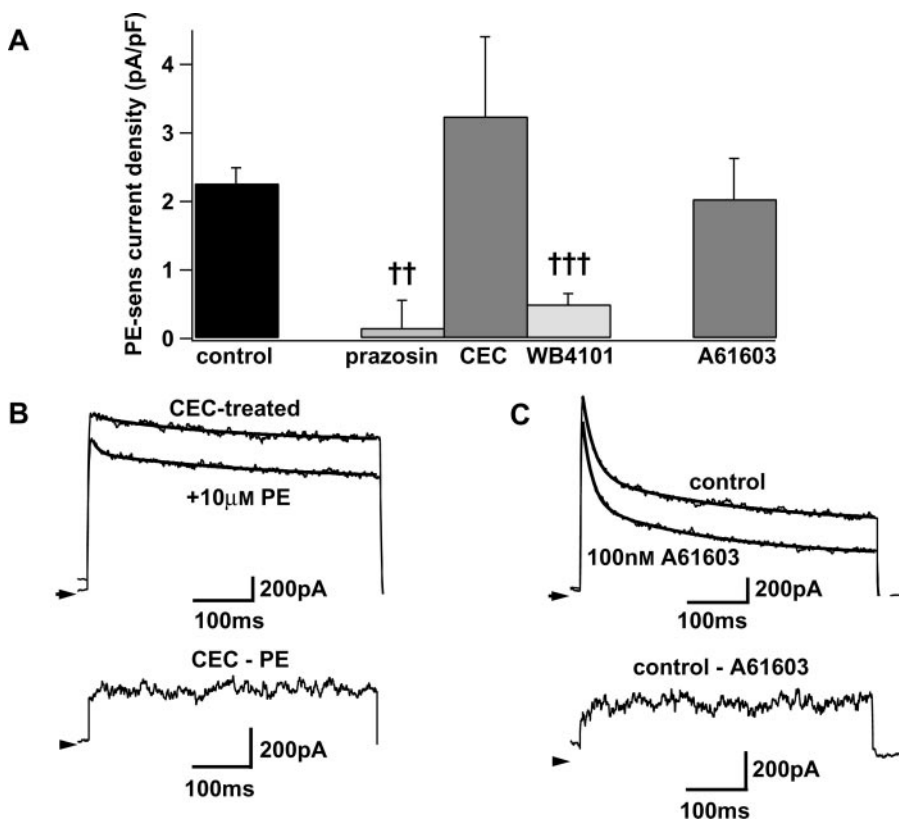


Fig. 11. The response to PE is mediated predominantly by α_{1A} -adrenoceptors. A, mean \pm S.E.M. of PE-sensitive current amplitudes under control conditions ($n = 44$), in the presence of 1 μ M prazosin ($n = 7$), and after pretreatment with 30 μ M CEC ($n = 5$), 100 nM WB4101 ($n = 6$), and the A61603-sensitive difference current ($n = 8$). ††, $p < 0.01$, unpaired t test with control; †††, $p < 0.001$, unpaired t test with control. Control A_0 was not significantly affected by either 1 μ M prazosin or 100 nM WB4101. The response to 10 μ M PE was not significantly reduced by a lower concentration (1 nM) of the competitive antagonist prazosin (1.62 ± 0.45 pA/pF, $n = 5$). B, top, example current traces from a cell pretreated with 30 μ M CEC before and after superfusion with 10 μ M PE. Solid lines represent fits to a double exponential equation. Lower shows PE-sensitive difference current. C, top, example current traces before and after superfusion with 100 nM A61603. Solid lines represent fits to a double exponential equation. Bottom, A61603-sensitive difference current.

is consistent with this conclusion (Fig. 12A). The results with U73122 and U73343 and the lack of effect of neomycin suggest that the actions of PE did not involve PLC or phospho-

lipase D, consistent with the observation of robust responses to PE when bulk cytosolic Ca²⁺ was chelated to <1 nM with BAPTA (Singer et al., 1997). Because AACOCF₃ is known to have nonspecific actions independent of PLA₂ inhibition (Fonteh, 2002) and MAFF had no significant effect on the responses to PE (Fig. 12B), there is no consistent evidence for the involvement of PLA₂. On the other hand, the inhibitory effect of wortmannin on the PE response suggests the involvement of PI 3-kinase (Fig. 12C).

Conclusions and Implications

It is well established that α_1 -AR stimulation modulates the electrophysiology of cardiac myocytes from different regions of the heart in a number of species (e.g., dog, ferret, rabbit, rat, human etc.), including rat ventricular myocytes (Fedida et al., 1993a; Li et al., 1996). Because I_{ss,PE} represented the predominant current modulated by α_1 -ARs in the present study, it seems likely to play an important role in the modulation of excitability and refractoriness in these cells. This current could therefore represent a potential target for antiarrhythmic agents, and further work is warranted to establish the contribution of this Slick-like K⁺ channel current to cardiac excitability and repolarization.

Acknowledgments

We thank Dr. Zhiwei Cai (Bristol) for discussion of noise analysis.

References

- Aimond F, Rauzier J-M, Bony C, and Vassort G (2000) Simultaneous activation of p38 MAPK and p42/44 MAPK by ATP stimulates the K⁺ current I_{TREK} in cardiomyocytes. *J Biol Chem* 275:39110–39116.
- Apkon M and Nerbonne JM (1991) Characterization of two distinct depolarization-activated K⁺ currents in isolated adult rat ventricular myocytes. *J Gen Physiol* 97:973–1011.
- Backx PH and Marban E (1993) Background potassium current active during the plateau of the action potential in guinea pig ventricular myocytes. *Circ Res* 72: 890–900.
- Barbuti A, Ishii S, Shimizu T, Robinson RB, and Feinmark SJ (2002) Block of the background K⁺ channel TASK-1 contributes to arrhythmogenic effects of platelet-activating factor. *Am J Physiol* 282:H2024–H2030.
- Bhattacharjee A, Joiner WJ, Wu M, Yang Y, Sigworth FJ, and Kaczmarek LK (2003) Slick (Slo2.1), a rapidly-gating sodium-activated potassium channel inhibited by ATP. *J Neurosci* 23:11681–11691.
- Czirjak G and Enyedi P (2003) Ruthenium red inhibits TASK-3 potassium channel by interconnecting glutamate 70 of the two subunits. *Mol Pharmacol* 63:646–652.
- Dempster J (1993) Analysis of ionic current fluctuations: noise analysis, in *Computer Analysis of Electrophysiological Signals*, pp 191–203, Academic Press, London.
- Despa S, Islam MA, Pogwizd SM, and Bers DM (2002) Intracellular [Na⁺] and Na⁺ pump rate in rat and rabbit ventricular myocytes. *J Physiol (Lond)* 539:133–143.
- Duprat F, Lesage F, Fink M, Reyes R, Heurteaux C, and Lazdunski M (1997) TASK, a human background K⁺ channel to sense external pH variations near physiological pH. *EMBO (Eur Mol Biol Organ) J* 16:5464–5471.
- Ertl R, Jähnel U, Nawrath H, Carmeliet E, and Vereecke J (1991) Differential electrophysiological and inotropic effects of phenylephrine in atrial and ventricular heart muscle preparations from rats. *Naunyn-Schmiedeberg's Arch Pharmacol* 344:574–581.
- Fedida D, Bouchard R, and Chen FS (1996) Slow gating charge immobilization in the human potassium channel Kv1.5 and its prevention by 4-aminopyridine. *J Physiol (Lond)* 494:377–387.
- Fedida D, Braun AP, and Giles WR (1993a) α_1 -adrenoceptors in myocardium: functional aspects and transmembrane signaling mechanisms. *Physiol Rev* 73:469–487.
- Fedida D, Wible B, Wang Z, Fermini B, Faust F, Nattel S, and Brown AM (1993b) Identity of a novel delayed rectifier current from human heart with a cloned K⁺ channel current. *Circ Res* 73:210–216.
- Fonteh AN (2002) Differential effects of arachidonyl trifluoromethyl ketone on arachidonic acid release and lipid mediator biosynthesis by human neutrophils: evidence for different arachidonate pools. *European J Biochem* 269:3760–3770.
- Helliwell RM and Large WA (1998) Facilitatory effect of Ca²⁺ on the noradrenaline-evoked cardiac current in rabbit portal vein smooth muscle cells. *J Physiol (Lond)* 512:731–741.
- Himmel HM, Wettwer E, Li Q and Ravens U (1999) Four different components contribute to outward current in rat ventricular myocytes. *Am J Physiol* 277: H107–H118.
- Homma N, Hirasawa A, Shibata K, Hashimoto K, and Tsujimoto G (2000) Both α_{1A} -

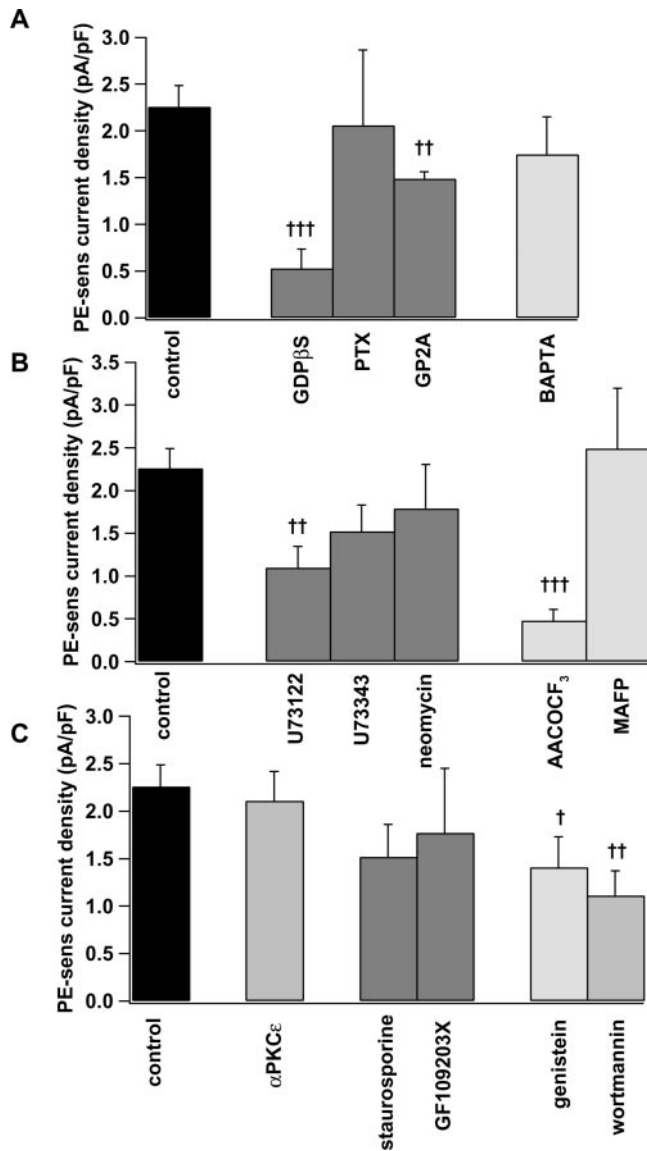


Fig. 12. The response to PE is mediated by a Ca²⁺-independent pathway involving a PTX-insensitive G-protein and PI 3-kinase. A, mean \pm S.E.M. of PE-sensitive current from control cells ($n = 44$), from cells dialyzed with a pipette solution containing 1 mM GDPβS ($n = 7$), from cells pretreated with 7.5 μ g/ml PTX ($n = 5$), from cells dialyzed with a pipette solution containing 10 μ M GP2A ($n = 5$), and from cells dialyzed with a nominally Ca²⁺-free pipette solution containing 10 mM BAPTA ($n = 7$). ††, $p < 0.01$, unpaired t test versus control; †††, $p < 0.001$, unpaired t test versus control. B, mean \pm S.E.M. of PE-sensitive current from cells treated with phospholipase inhibitors. Cells were pretreated with 5 μ M U73122 ($n = 5$), 5 μ M U73343 ($n = 11$), 2 mM neomycin sulfate ($n = 5$), 40 μ M AACOCF₃ ($n = 8$), or 25 μ M MAFF ($n = 4$). ††, $p < 0.01$, unpaired t test versus control; †††, $p < 0.001$, unpaired t test versus control. C, mean \pm S.E.M. of PE-sensitive current in cells treated with various kinase inhibitors. The PKCε-specific peptide antagonist (αPKCε; 75 μ M, $n = 3$) and wortmannin (5 μ M, $n = 5$) were applied via the pipette solution. Cells were pretreated for 30 min with 200 nM staurosporine ($n = 4$), 1 μ M GF109203X ($n = 5$), and 50 μ M genistein ($n = 7$). †, $p < 0.05$, unpaired t test versus control; ††, $p < 0.01$, unpaired t test versus control. GDPβS, GP2A, U73122, AACOCF₃, and wortmannin had no significant effect on the control current. However, the control current was significantly inhibited by genistein (from 4.83 ± 0.36 to 3.22 ± 0.40 pA/pF, $p < 0.001$, $n = 7$).

- and $\alpha_1\text{B}$ -adrenergic receptor subtypes couple to the transient outward current (I_{To}) in rat ventricular myocytes. *Br J Pharmacol* **129**:1113–1120.
- Jones SA, Morton MJ, Hunter M, and Boyett MR (2002) Expression of TASK-1, a pH-sensitive twin-pore domain K^+ channel, in rat myocytes. *Am J Physiol* **283**:H181–H185.
- Kim Y, Bang H, and Kim D (1999) TBAK-1 and TASK-1, two-pore K^+ channel subunits: kinetic properties and expression in rat heart. *Am J Physiol* **277**:H1669–H1678.
- Leonoudakis D, Gray AT, Winegar BD, Kindler CH, Harada M, Taylor DM, Chavez RA, Forsayeth JR, and Yost CS (1998) An open rectifier potassium channel with two pore domains in tandem cloned from rat cerebellum. *J Neurosci* **18**:868–878.
- Lesage F and Lazdunski M (2000) Molecular and functional properties of two-pore-domain potassium channels. *Am J Physiol* **279**:F793–F801.
- Li G-R, Feng J, Wang Z, Fermini B, and Nattel S (1996) Adrenergic modulation of ultrarapid delayed rectifier K^+ current in human atrial myocytes. *Circ Res* **78**:903–915.
- Liscovitch M, Chalifa V, Danin M, and Eli Y (1991) Inhibition of neural phospholipase D activity by aminoglycoside antibiotics. *Biochem J* **279**:319–321.
- Maingret F, Patel AJ, Lazdunski M, and Honore E (2001) The endocannabinoid anandamide is a direct and selective blocker of the background K^+ channel TASK-1. *EMBO (Eur Mol Biol Organ) J* **20**:47–54.
- Millar JA, Barratt L, Southan AP, Page KM, Fyffe REW, Robertson B, and Mathie A (2000) A functional role for the two-pore domain potassium channel TASK-1 in cerebellar granule neurons. *Proc Natl Acad Sci USA* **97**:3614–3618.
- Moss BL and Magleby KL (2001) Gating and conductance properties of BK channels are modulated by the S9–S10 tail domain of the α subunit: a study of mSlo1 and mSlo3 wild-type and chimeric channels. *J Gen Physiol* **118**:711–734.
- Mukai H, Munekata E, and Higashijima T (1992) G protein antagonists. A novel hydrophobic peptide competes with receptor for G protein binding. *J Biol Chem* **267**:16237–16243.
- Nattel S, Yue L, and Wang Z (1999) Cardiac ultrarapid delayed rectifiers: a novel potassium current family of functional similarity and molecular diversity. *Cell Physiol Biochem* **9**:217–226.
- Patel AJ, Honore E, Maingret F, Lesage F, Fink M, Duprat F, and Lazdunski M (1998) A mammalian two pore domain mechano-gated S-like K^+ channel. *EMBO (Eur Mol Biol Organ) J* **17**:4283–4290.
- Ravens U, Wang X-L, and Wettwer E (1989) α -Adrenoceptor stimulation reduces outward currents in rat ventricular myocytes. *J Pharmacol Exp Ther* **250**:364–370.
- Shahidullah M, Hoshi N, Yokoyama S, Kawamura T, and Higashida H (1995) Slow inactivation conserved in heteromultimeric voltage-dependent K^+ channels between Shaker (Kv1) and Shaw (Kv3) subfamilies. *FEBS Lett* **371**:307–310.
- Shieh CC and Kirsch GE (1994) Mutational analysis of ion conduction and drug binding sites in the inner mouth of voltage-gated K^+ channels. *Biophys J* **67**:2316–2325.
- Singer WD, Brown HA, and Sternweis PC (1997) Regulation of eukaryotic phosphatidylinositol-specific phospholipase C and phospholipase D. *Annu Rev Biochem* **66**:475–509.
- Snyders DJ (1999) Structure and function of cardiac potassium channels. *Cardiovasc Res* **42**:377–390.
- Taglialatela M, Champagne M, Drewe J, and Brown A (1994) Comparison of H5, S6 and H5–S6 exchanges on pore properties of voltage-dependent K^+ channels. *J Biol Chem* **269**:13867–13873.
- Talley EM, Lei Q, Sirois JE, and Bayliss DA (2000) TASK-1, a two-pore domain K^+ channel, is modulated by multiple neurotransmitters in motoneurons. *Neuron* **25**:399–410.
- Terrenoire C, Lauritzen I, Lesage F, Romey G, and Lazdunski M (2001) A TREK-1-like potassium channel in atrial cells inhibited by β -adrenergic stimulation and activated by volatile anesthetics. *Circ Res* **89**:336–342.
- van Wagoner DR, Kirian M, and Lamorgese M (1996) Phenylephrine suppresses outward K^+ currents in rat atrial myocytes. *Am J Physiol* **271**:H937–H946.
- Wang H, Yang B, Zhang Y, Han H, Wang J, Shi H, and Wang Z (2001) Different subtypes of α_1 -adrenoceptor modulate different K^+ currents via different signaling pathways in canine ventricular myocytes. *J Biol Chem* **276**:40811–40816.
- Zhong H and Minneman KP (1999) α_1 -Adrenoceptor subtypes. *Eur J Pharmacol* **375**:261–276.

Address correspondence to: Dr. Andrew F. James, Department of Physiology and Cardiovascular Research Laboratories, School of Medical Sciences, University of Bristol, University Walk, Bristol, BS8 1TD, United Kingdom. E-mail: a.james@bristol.ac.uk